Astronomical and Astrophysical Transactions (*AApTr*), 2014, Vol. 28, Issue 4, pp. 317–330,
ISSN 1055-6796, Photocopying permitted by license only, ©Cambridge Scientific Publishers

Straight segments in the stellar disks

A.M. Mel'nik[1*], P. Rautiainen[2†]

[1] *Sternberg Astronomical Institute, Lomonosov Moscow State University, 13 Universitetskij pr., Moscow 119992, Russia*
[2] *Department of Astronomy and Space Physics, University of Oulu, P.O. Box 3000, FIN-90014 Oulun yliopisto, Finland*

Received 13 October, 2013

We study the properties of the straight segments forming in N-body simulations of the galactic stellar disks. The straight segments are supposed to appear as a response of the rotating disk to a gravity of the regions of enhanced density (overdensities). The kinematics of stars near the prominent overdensities is consistent with this hypothesis. The possible mechanisms of the formation of overdensities are discussed.

Keywords: Galaxies: kinematics and dynamics – galaxies: spiral – galaxies: structure

1 Introduction

Straight segments outline the spiral structure of many galaxies, as it is, for example, in M101 and in M51, forming polygonal spiral arms (Chernin et al. 2000). Probably, the straight segments were first noticed by B. Lindblad who paid attention to sudden bends in the spiral arms of M51 (Lindblad 1936, Fig. 17). Vorontsov-Vel'yaminov (1978) discovered straight segments in many galaxies. He was first who realized that straight segments, which he called rows, are a wide-spread phenomenon.

Though straight segments are more prominent in the young stellar population, they can also form in the old stellar disks. Our inspection of the near-IR images of Ohio State University Bright Spiral Galaxy Survey (Eskridge et al. 2002) revealed that in more than half of the cases, the straight segments observed in the B-band had their counterparts also in the H-band (Fig. 1). The straight segments are also quite conspicuous in the near-infrared J- and K-band images of galaxies NGC 3938 and NGC 4254 obtained by Castro-Rodriguez & Garzon (2003). The bands J, H, K are situated near 2 μm where the main contribution comes from the old disk stars (K2–K3 III).

Chernin et al. (2001) compile the catalog of galaxies with straight segments that includes about 200 objects. They have found that length of the straight segment L

*Email: anna@sai.msu.ru
†Email: pertti.rautiainen@oulu.fi

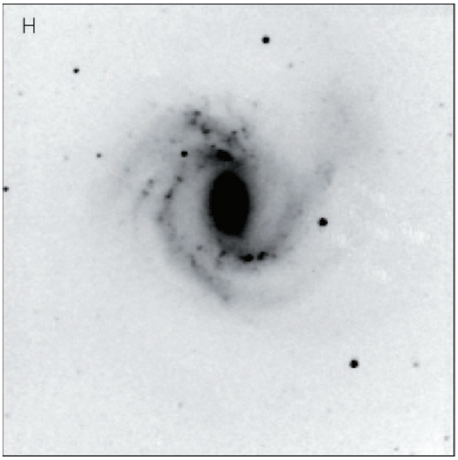

Figure 1 The H-band image of the galaxy NGC 4303 from the Ohio State University Sample of Bright Galaxies (Eskridge at al. 2002).

increases with the galactocentric distance R, so that $L = (1 \pm 0.13)R$. They also show that the angle α between two neighboring straight segments has the average value of 120° with the standard deviation of $\sim 10^\circ$.

Khoperskov at al. (2011) and Filistov (2012) model straight segments in the gaseous disks under the given analytical potential. They explain the formation of the straight segments by pure gas dynamical effects there (see also Chernin 1999).

As for stellar disks, there are two different approaches to explain the formation of ragged polygonal spiral arms in the stellar component: one is based on the global modes (Toomre 1981) and the other rests on the chaotically distributed density perturbations (Toomre & Kalnajs 1991).

Toomre (1981) explains the square-like shape of the spiral arms by the presence of the leading and trailing spiral waves of nearly similar wavelengths and amplitudes in the Fourier spectrum of the mode, where the leading wave appears due to reflection of the in-going trailing wave from the center (Athanassoula 1984, Binney & Tremaine 2008, for more details). But it is not clear how the superposition of the leading and trailing waves on the galactic periphery is produced.

In the other approach the observed spiral structure is considered as a set of arm features forming due to random density fluctuations in galactic disks (Toomre 1990). Julian & Toomre (1966) consider the response of the stellar disk to a chance overdensity (a large clump of gas) corotating with the disk. The density response can exceed the initial perturbation more than several tens times (Goldreich & Lynden-Bell 1965; Julian & Toomre 1966; Toomre 1981). This mechanism called swing amplification is based on the concerted action of noise, epicyclic motion, and self-gravity (Toomre 1981). Sellwood & Carlberg (1984) study the work of the swing amplification mechanism and show that the maximal amplification is possible on the galactic periphery for the multi-armed spiral patterns.

D'Onghia, Vogelsberger, & Hernquist (2013) carried out some numerical experiments with stellar disks and have shown that the system of disturbers ($M \approx 10^6\ M_\odot$)

corotating with the disk gives rise to the formation of the multi-armed polygonal spiral arms (or linear segments joined at kinks).

Recently, many researchers have noted that the multi-armed spiral structure in their N-body simulations doesn't rotate as a whole, but consists of pieces corotating with the disk at different radii (Wada, Baba, & Saitoh 2011; Grand, Kawata, & Cropper 2012; Baba, Saitoh, & Wada 2013; D'Onghia, Vogelsberger, & Hernquist 2013, Roca-Fàbrega et al. 2013).

In this paper we study properties of the straight segments forming in N-body galactic disks. We show that the features of the model straight segments are in good agreement with the observational ones summarized by Chernin at al. (2001). We suggest that the straight segments are forming as a response of the rotating disk to a gravity of the regions of enhanced density (overdensities) corotating with the disk. The properties of these respondent perturbations can explain the observational features of the straight segments (for more details, see Mel'nik & Rautiainen 2013). The possible mechanisms of the formation of overdensities are discussed.

2 The properties of the disk response to the overdensity

2.1 The shape of the respondent perturbation

Toomre (1964) has shown that the stability of the disk is supported by shared action of the equivalent of pressure resulting from random motions and the Coriolis forces: the pressure effectively suppresses perturbations on the short side of wavelengths, while the Coriolis forces suppress instabilities on the long end. The value of λ_c is the shortest wavelength of axisymmetric perturbations that can be stabilized by epicyclic motions only:

$$\lambda_c = \frac{4\pi^2 G\Sigma}{\kappa^2}, \tag{1}$$

where Σ is the surface density of the disk and κ is the epicyclic frequency.

Julian & Toomre (1966) consider the response of a thin differentially rotating stellar disk to the presence of a single, particle-like concentration of the interstellar matter (overdensity) corotating with the disk. They have found that overdensity creates quite extended spiral-like density response in the disk: the size of the density ridge in the radial direction amounts $\sim\lambda_c/2$.

Figure 2 shows the trajectory of a star with respect to the initial overdensity that is obtained without taking into account the self-gravity (Julian & Toomre 1966). The star in question is located at the larger distance than the disturber, and first it has purely circular velocity. In the reference frame corotating with the disturber the star moves in the direction opposite that of galactic rotation, i.e. clockwise. In the impulse approximation star's angular momentum is unchanged and its motion can be thought as a superposition of the purely circular motion and the motion along the epicycle (Binney & Tremaine 2008). Let us suppose that the star gains some impulse and starts its epicyclic motion when the distance between the star and the disturber is minimal, i.e. when the star and the disturber are lying at the same radius-vector. The moment of start of the epicyclic motion is denoted by number "1" and corresponds to

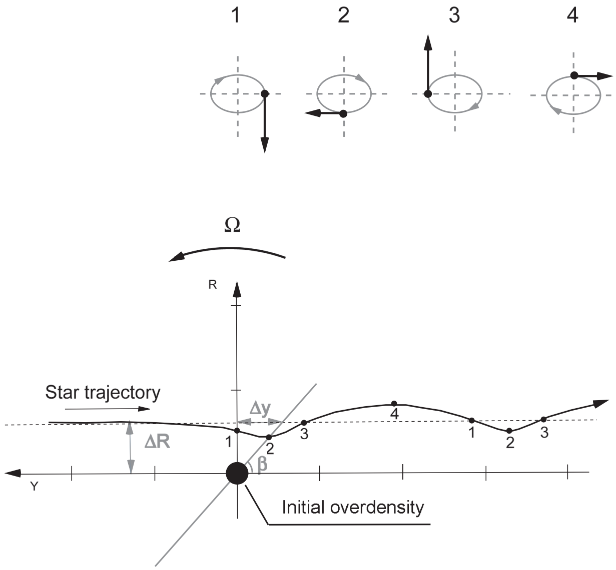

Figure 2 The trajectory of the star (black curve) perturbed by the initial overdensity (Julian & Toomre 1966). The motion is considered in the reference frame corotating with the initial disturber that lies in the origin and rotates with circular velocity. The star in question is lying at a distance larger than that of the disturber and initially moves with purely circular velocity. In the chosen reference frame it moves in the sense opposite to that of galactic rotation, i.e. clockwise. Numbers 1–4 denote positions of the star at moments separated by 1/4 of the epicyclic period. The upper row shows the position of the star in the epicyclic orbit at moments 1–4. Gray line indicates position of the straight segment without taking its self-gravity into account.

the maximal additional velocity directed toward the galactic center. Julian & Toomre (1966) suggest that the resulting stellar density must be the greatest wherever the individual stars linger longest. That moment denoted by number "2" occurs in nearly one-quarter of the epicyclic period, when the star has the maximal additional velocity directed in the sense of galactic rotation. Note that in the chosen reference frame, the star in question moves in the direction opposite that of galactic rotation, so the moment with the largest velocity in the sense of galactic rotation determines the place there the star lingers most. Moment "3" corresponds to the maximal additional velocity directed away from the galactic center. The additional velocity in moment "4" is directed in the sense opposite that of galactic rotation.

Let us calculate an angle β which determines the position of the respondent perturbation with respect to the azimuthal direction. In the first approximation we neglect the additional velocities due to the epicyclic motions. Then the distance Δy which is passed by the star with respect to the initial disturber during one-quarter of the epicyclic period $\pi/(2\kappa)$ is determined by the relation:

$$\Delta y = |\Omega(R) - \Omega(R_0)| \frac{\pi R_0}{2\kappa}, \tag{2}$$

And for the flat rotation curve ($\Omega(R) = V_0/R$, $\kappa = \sqrt{2}\Omega$) we can express the angle β in the following form:

$$\beta = \arctan \frac{2\sqrt{2}}{\pi} = 42^\circ, \tag{3}$$

which is very close to the value $\sim 45^\circ$ suggested by Julian & Toomre (1966) for flat rotation curve.

Generally, the fact that the angle β is independent from the coordinates ΔR and Δy suggests that the stellar response has the shape of a straight line. However, the impulse approximation isn't accurate, especially in the very vicinity of the initial disturber, because any star during the approach phase of the encounter changes its angular momentum and passes the disturber with a slower relative velocity than it would be without interaction (Julian & Toomre 1966).

Note that in the vicinity of the disturber, stars oscillate conspicuously in the radial direction moving first toward the disturber and then away from it. And the star can continue its radial oscillations as it moves in the azimuthal direction.

In the disks with low parameter Q (but $Q > 1$) self-gravity plays an important role (Toomre 1981), so after some moment the stellar trajectories are rather determined by the gravity of the straight segment itself than by the initial disturber.

Let us again consider the motion of the star initially moving on the circular orbit (Fig. 2). The self-gravity effects are maximal at the time interval when the star is leaving the straight segment and is moving nearly parallel to it. In Fig. 1 it is a path between points "2" and "3". Due to the gravity of the straight segment the position of the density maximum is shifting in the direction of the point "3", because here the star has maximal value of the radial velocity which allows it to move along the straight segment during the longest period of time.

Using the approach described above we can calculate the pitch angle of the self-gravitating straight segment which must be nearly two times smaller than the angle calculated without self-gravity:

$$\beta = \arctan \frac{\sqrt{2}}{\pi} = 24^\circ. \tag{4}$$

Julian & Toomre (1966) calculated the disk response to the initial disturber with and without self-gravity (Figs. 7 and 12 in Julian & Toomre 1966, correspondingly). Comparison of the disk response in the two cases suggests that the self-gravity effects conduce to the density response being more linear-shaped.

2.2 The length of the straight segments

The most interesting parameter is the linear size of the respondent density perturbation. Julian & Toomre (1966) show that the size of the density ridge in radial direction is $\Delta R \approx \lambda_c/2$. This result is expected because $\lambda_c/2$ is the maximal radial size of the region with the density above the average in the marginally stable axisymmetric oscillations (Toomre 1964).

Let us compare the value of λ_c with the radius R at which it is calculated (see also Fig. 5a in Toomre 1977). We can approximate the distribution of the disk density using the relation:

$$\Sigma \approx \frac{f_d V_0^2}{2\pi G R}, \tag{5}$$

where V_0 is the velocity of the rotation curve and f_d is the contribution of the disk to the total rotation curve. Using Eq. 1 and the relations $\kappa = \sqrt{2}\Omega$, $\Delta R \approx \lambda_c/2$ we obtain:

$$\Delta R \approx \pi f_d R/2. \tag{6}$$

Then the full size of the straight segment L under the angle $\beta \approx 42°$ must be following:

$$L \approx 2.4 f_d R. \tag{7}$$

Here we suppose that the self-gravity effects can not significantly increase the linear size of the straight segments.

The value of f_d in the distance range considered in our models lies in the range $f_d = 0.3$–0.5. So the maximal possible length of the straight segment must lie in the range $L = (0.7$–$1.2)R$. On the whole, this result is consistent with the observations (Chernin et al. 2001).

3 Models

The N-body simulations used in this article were done by applying the code written by H. Salo (Salo 1991; Salo & Laurikainen 2000). The stellar disk is self-gravitating, but the bulge and halo are analytical. The gas component is omitted in this paper.

We have made a large set of N-body models to study the formation and evolution of straight segments in the galactic disks. In these models we varied several parameters such as the mass fractions of different components, the value of the initial Toomre-parameter of the disk, the extent of the disk and the value of the gravitational softening parameter (Plummer-softening). Here we discuss the results of one selected model.

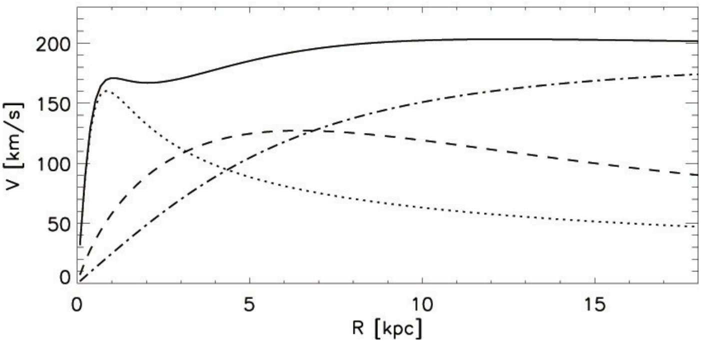

Figure 3 The rotation curve of the selected model. The continuous line shows the total rotation curve, the bulge contribution is drawn with a dotted line, the disk contribution with a dashed line and the halo contribution with a dash-dotted line.

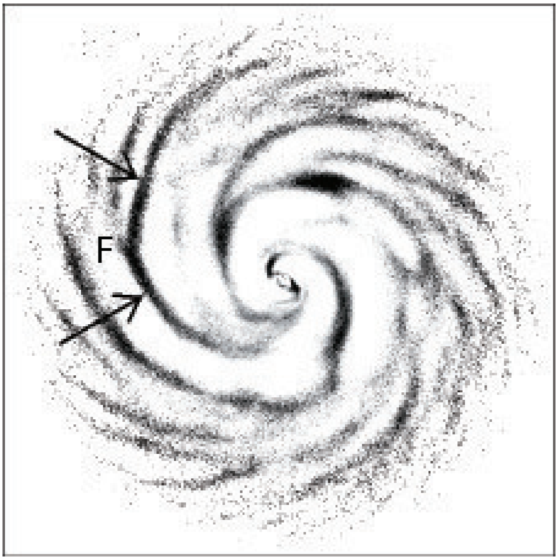

Figure 4 The stellar density enhancement above the average value in the model galactic disk at $T = 591.25$ Myr. The width of the frame is 18 kpc. The two arrows show the locations of two straight segments considered with a point of their contact designated by "F".

The rotation curve of our model is shown in Fig. 3, with the adopted physical scaling of the simulation units. The disk particles were originally distributed as an exponential disk with scale length $R_e = 3.0$ kpc. The mass of the disk is $M_\mathrm{d} = 2.9 \times 10^{10}\ M_\odot$. The bulge component was modelled as an analytical Plummer sphere with the mass of $M_\mathrm{b} = 9.2 \times 10^9\ M_\odot$ and scale length of $b = 0.6$ kpc. The analytical halo was of the same form as in Rautiainen & Melnik (2010). The asymptotic rotation velocity of the halo equals 189 km s^{-1} that with core radius of $R_C = 7.5$ kpc gives the mass of halo within 15 kpc of $M_\mathrm{h} = 9.9 \times 10^{10}\ M_\odot$. The model is mostly dominated by the spherical (analytical) component (bulge and halo); the reason for this choice of parameters was to delay bar formation but the initial value of the Toomre-parameter is low enough ($Q_T = 1.2$) that it still allows the disks to develop well-defined spiral arms. The gravitational softening is $\epsilon = 75$ pc.

The model first develops a multiple-armed structure. In the outer parts of the disk there are $m = 10$–20 short arms. The structure becomes more regular in the inner parts, but even there the number of arms amounts to $m = 2$–5. A large scale bar forms at $T \approx 800$ Myr. After its formation, the inner spiral structure becomes effectively two-armed and the number of spiral arms also diminish in the outer parts, although it still remains multiple-armed.

Figure 4 shows the density enhancement above the average value in the model galactic disk at $T = 591.25$ Myr. We chose two straight segments and followed their evolution. They were selected because they are exceptionally long-lived, lasting about 80 Myr, which corresponds to about 1/4 of the circular rotation period at the radial distance of the segments. Most straight segments seen in our models have shorter lifespans corresponding to 10–30 Myr.

4 General characteristics of straight segments in model disks

We have identified 238 straight segments in model stellar disk at different time moments. The changes of the length of the model straight segments L along radius R are shown in Fig. 5. The galactocentic distance R for the straight segment is determined as the distance to its median point. The thick gray curve shows the value of L calculated from the formula $L = 2.4 f_d R$, where $f_d(R)$ is the relative contribution of the disk to the total rotation curve at each radius. The value of $f_d(R)$ achieves the maximum at $R \sim 2R_e$ and then gradually decreases with increasing R (Fig. 6).

The linear dependence $L = (0.86 \pm 0.02)R$ derived for the model straight segments is consistent with observational one $L = (1.0 \pm 0.13)R$. However, the connection between L and R in the model disk is conspicuously non-linear: there are a lot of relatively short straight segments at large radii. So the connection between L and R is better described by formula $L = 2.4 f_d R$ which gives the standard deviation of $\sigma = 1.54$ kpc instead of $\sigma = 2.1$ kpc obtained for the linear law.

Since the straight segments rotate in the disk with the angular velocity of their parent overdensities, they can never form stationary polygonal structure. Moreover, straight segments must destroy each other during their merging. The only possible way for their contact without destruction is by touching of their edges. In this case they can even increase each other because the appearance of the extra density at their endpoints gives both of them an extra ability to hold stars inside them.

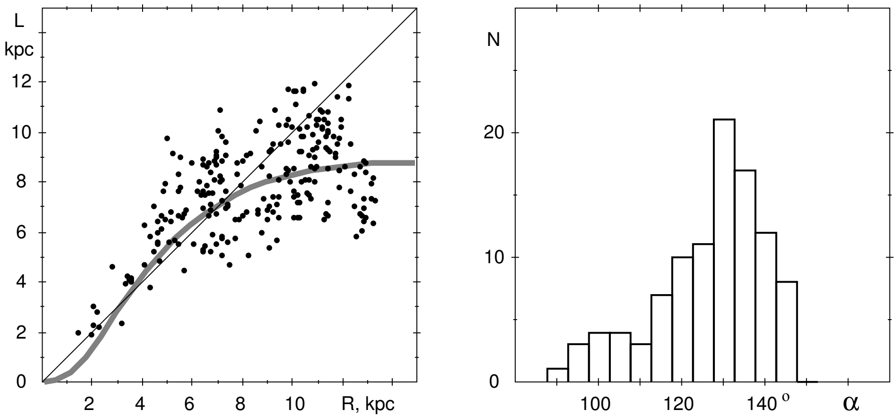

Figure 5 Left panel: the dependence between the length L of a model straight segment and its galactocentric distance R. The thick gray curve shows the value of L calculated from the formula $L = 2.4 f_d R$. The bisectrix is also drawn. Right panel: the histogram of the distribution of the angle α between two neighboring straight segments in the model disk.

We measured 101 angles between neighboring straight segments in model disk. Its average value appears to be $\overline{\alpha} = 127°$ with the standard deviation of $\sigma = 13°$. The maxima of distribution of α lies $\sim$130° (Fig. 6). All these values are consistent with observations.

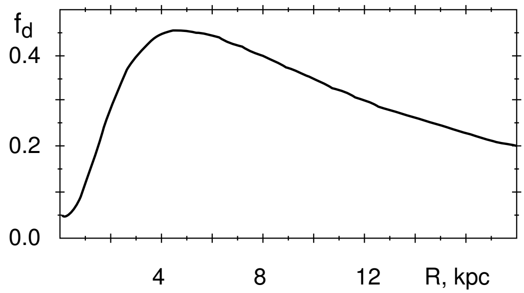

Figure 6 The variation of f_d – the relative contribution of the disk to the total rotation curve (v_c^2) – along the radius in model disk.

Chernin (1999) gives an explanation of the the value of $\overline{\alpha} = 120°$ which is based on the relation $L = R$. Using the relation $L = 0.86R$ we can explain why the value of α in our model equals $\overline{\alpha} = 127°$ (for more details see Melnik & Rautiainen 2013).

5 Kinematical features of the straight segments

The role of the initial overdensities in production of the straight segments is to adjust the epicyclic motions of stars passing by. So the overdensities must create the specific velocity field in their neighborhood.

In a case when both the gravity of the initial disturber and self-gravity of the straight segment are important we can expect that the conspicuous gradient of the radial and azimuthal velocities in the straight segments near overdensities and its direction must be following: the larger (smaller) R, the more positive (negative) value of V_R or V_T (Fig. 2).

To study the kinematics of stars in our models we calculate the residual velocities of stellar particles in the radial and azimuthal directions, V_R and V_T. In our previous paper (Rautiainen & Melnik 2010) we determined V_R and V_T as differences between the model velocities and the velocity due to rotation curve, but here we compute the velocity V_T with respect to the average azimuthal velocity of stellar particles at the same radius but not with respect to the rotation curve.

To study the kinematics in the model disks we divide them into small squares with the size of 150×150 pc and calculate the average radial and azimuthal residual velocities, V_R and V_T, for stars located inside them. Figure 7 exhibits the distribution of the negative and positive residual velocities, V_R and V_T, averaged in squares at $T = 632.50$ Myr. We also denote the positions of the most prominent overdensities having the density twice the average one, $n/n_0 > 2$, where n is the number of particles in a square and n_0 is the average number of particles in squares at the same radius. Let us consider the distribution of the velocities near two overdensities designated by letters "A" and "B". We can see the conspicuous gradients of the velocities, V_R or V_T, near the overdensity "B" and the sense of changes coincides with the expected one: the larger (smaller) R, the more positive (negative) value of V_R or V_T. As for the overdensity "A", the azimuthal velocities V_T near it demonstrate the expected

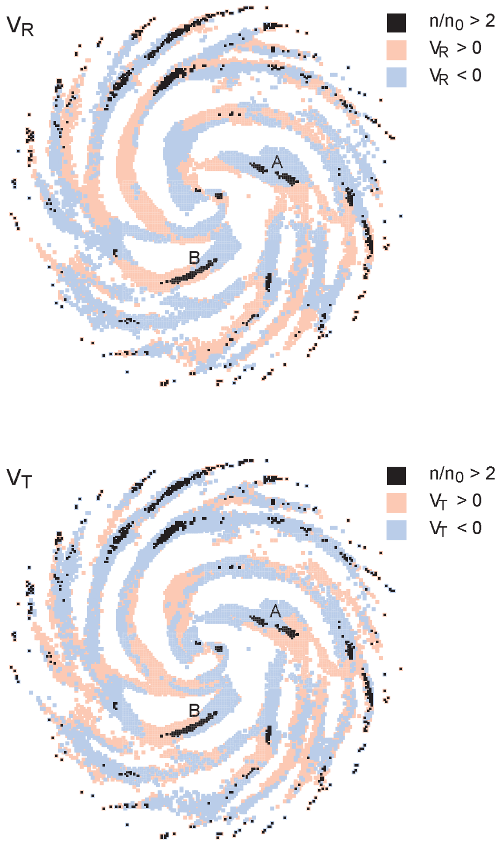

Figure 7 The distribution of the radial V_R and azimuthal V_T residual velocities averaged in small squares. Squares with positive velocities, V_R or V_T, are shown in red, while squares with negative velocities are given in blue. It also exhibits the distribution of overdensities with $n/n_0 > 2$ (black squares). Two overdensities are designated by letters "A" and "B". The gradient of the velocities, V_R or V_T, near them is expected to be the following: the larger (smaller) R, the more positive (negative) velocity.

velocity gradient (the lower image), while the radial velocities V_R do not, but at the next moment considered, $T = 646.25$, they already exhibit the expected velocity gradient. Note that the arrangement of the azimuthal velocities occurs earlier than that of the radial ones (for more details, see Mel'nik & Rautiainen 2013).

6 Conclusions and discussion

We consider the formation of the straight segments in the stellar galactic disks. For this purpose we constructed several N-body simulations and identified straight segments there. The straight segments are temporal features which rotate with the average velocity of the disk. The relation between the length L of the model straight segment and its galactocentric distance R can be approximated by the linear law $L = (0.86 \pm 0.02)R$. The average angle between two neighboring straight segments in our model appears to be $\overline{\alpha} = 127°$. All these values are consistent with the observational estimates, $L = (1.0 \pm 0.13)R$ and $\alpha = 120°$, derived by Chernin et al. (2001).

We suggest that the formation of the straight segments in stellar disks is connected with the appearance of the overdensities corotating with the disk. In the first approximation the response of the stellar disk to such overdensity must have the shape of a straight segment with the length determined by the formula $L = 2.4 f_d R$. Comparison of the average characteristics of the model straight segments with the parameters of the respondent perturbations shows that the non-linear relation $L = 2.4 f_d R$ describes better the connection between L and R than the linear one $L = kR$.

The study of the kinematics of stars near the most prominent overdensities reveals the specific velocity gradient near them: at the radii larger than that of the overdensity the velocities V_R and V_T are positive, while at the smaller radii they are negative. Such velocity field agrees with the hypothesis that the straight segments are forming due to the tuning of the epicyclic motions near the initial disturbers corotating with the disk. The amplitude of the velocity changes inside straight segments can achieve 10 km s^{-1} (for more detail, see Mel'nik & Rautiainen 2013).

The most interesting question is the nature of the overdensities bringing the formation of the straight segments. Julian & Toomre (1966) and D'Onghia et al. (2013) consider the giant molecular clouds with a mass of $\sim 10^6\ M_\odot$ as possible candidates for the role of overdensities disturbing the disk. But the observed giant molecular complexes have large internal velocity dispersion, which indicates their being unbound (Dame at al. 1986). For the formation of the straight segment the initial overdensity must survive at least during $\sim 1/4$ of the epicyclic period, which is needed for tuning epicyclic motions near it, then the effects of self-gravity start working and the role of the initial overdensity is decreasing. At the solar neighborhood 1/4 of the epicyclic period amounts to $\sim$ 30 Myr. It is questionable whether the giant molecular cloud can survive for such a long time period; first, a start of the star formation can destroy them much earlier; second, the growing straight segment forms forces which try to tear the initial overdensity.

We suppose that the appearance of such overdensities in our models is connected with the interaction of different density modes or waves. Edge modes being usually one- or two-armed (Tomre 1977, 1981) can also play some role in the formation of the overdensities. But even current density waves can accelerate the growth of one or two overdensities among many others located at the same radius. The competition among overdensities determines the leaders among them which can create organized radial oscillations of stars at some sector of the disk. These oscillations can strengthen other primordial overdensities located in "the right places", i.e. in the sites where stars pass by with the minimal azimuthal velocity (Fig. 2). Probably, the adjustment of the stellar motions in accordance with one or two of the most prominent overdensities situated at the same radius causes the formation of the quasi-regular spiral structure, otherwise, it must be chaotic.

Here we have considered the kinematics near a single overdensity corotating with the disk, however two straight segments touching each other by their ends usually exhibits a different velocity distribution. The distinction in the kinematics of a single and the interacting straight segments can be caused by the formation of the new overdensity in the point of contact of two straight segments (for example, the point "F" in Fig. 4), what is often observed in our models. Possibly, the ends of the straight segments can create some favorable conditions for the formation of the new overdensities.

Chernin at al. (2001) noted that the fraction of interacting galaxies among the galaxies with straight segments is appreciably higher than among galaxies without them. Possibly, the external perturbations can accelerate the process of the formation of the prominent overdensities in the middle part of the disk ($\sim 2R_e$).

Our modelling shows that the extended stellar disks favor the formation of the polygonal spiral arms. D'Onghia et al. (2013) also note that the response of the disk to the overdensity depends on the extent to which the disk is self-gravitating. The most simple explanation of this relation is the capability of the disk periphery to amplify significantly even small density noise (Sellwood & Carlberg 1984).

Acknowledgments

We wish to thank Heikki Salo for using his simulation code. This work made use of data from the Ohio State University Bright Spiral Galaxy Survey, which was funded by grants AST-9217716 and AST-9617006 from the United States National Science Foundation, with additional support from the Ohio State University. This work was supported in part by the Russian Foundation for Basic Research (project nos. 12-02-00827, 13-02-00203).

References

Athanassoula, E. (1984) *Phys. Rep.* **114**, 321

Baba, J., Saitoh, T. R., Wada, K. (2013) *Astrophys. J.* **763**, 46

Binney, J. and Tremaine, S. (2008) *Galactic Dynamics*, 2-nd edn. Princeton Univ. Press, Princeton, NJ

Castro-Rodríguez, N. and Garzón, F. (2003) *Astron. Astrophys.* **411**, 55

Chernin, A. D. (1999) *Mon. Not. R. Astron. Soc.* **308**, 321

Chernin, A. D., Kravtsova, A. S., Zasov, A. V., Arkhipova, V. P. (2001) *Astron. Reports* **45**, 841

Chernin, A. D., Zasov, A. V., Arkhipova, V. P., Kravtsova, A. S. (2000) *Astron. Lett.* **26**, 285

Dame, T. M., Elmegreen, B. G., Cohen, R. S., Thaddeus, P. (1986) *Astrophys. J.* **305**, 892

D'Onghia, E., Vogelsberger, M., Hernquist, L. (2013) *Astrophys. J.* **766**, 34

Eskridge, P. B., Frogel, J. A., Pogge, R. W. et al. (2002) *Astrophys. J. Suppl. Ser.* **143**, 73

Filistov, E. A. (2012) *Astron. Reports* **56**, 9

Goldreich, P. and Lynden-Bell, D. (1965) *Mon. Not. R. Astron. Soc.* **130**, 125

Grand, R.J., Kawata, D., Cropper, M. (2012) *Mon. Not. R. Astron. Soc.* **421**, 1529

Julian, W.H. and Toomre, A. (1966) *Astrophys. J.* **146**, 810
Khoperskov, S. A., Khoperskov, A. V., Eremin, M. A., Butenko, M. A. (2011) *Astron. Lett.* **37**, 563
Lindblad, B. (1936) *Stockholms Obs. Ann.* **12**, 4
Mel'nik, A. M. and Rautiainen, P. (2013) *Mon. Not. R. Astron. Soc.* **434**, 1362
Rautiainen, P. and Mel'nik, A. M. (2010) *Astron. Astrophys.* **519**, 70
Roca-Fàbrega, S., Valenzuela, O., Figueras, F., Romero-Gómez, M., Velázquez, H., Antoja, T., Pichardo, B. (2013) *Mon. Not. R. Astron. Soc.* **432**, 2878
Salo, H. (1991) *Astron. Astrophys.* **243**, 118
Salo, H. and Laurikainen, E. (2000) *Mon. Not. R. Astron. Soc.* **319**, 377
Sellwood, J. A. and Carlberg, R.G. (1984) *Astrophys. J.* **282**, 61
Toomre, A. (1964) *Astrophys. J.* **139**, 1217
Toomre, A. (1977) *Ann. Rev. Astron. Astrophys.* **15**, 437
Toomre, A. (1981) *The Structure and Evolution of Normal Galaxies,* Ed. by S.M. Fall, D. Lynden-Bell (Cambridge Univ. Press, Cambridge) p. 111
Toomre, A. (1990) *Dynamics and Interactions of Galaxies,* Ed. by R. Wielen (Springer-Verlag, Berlin, Heidelberg) p. 292
Toomre, A. and Kalnajs, A. J. (1991) *Dynamics of Disc Galaxies,* Ed. by B. Sundelius (Göteborgs Univ., Göthenburg) p. 341
Vorontsov-Vel'yaminov, B. A. (1978) *Extragalactic Astronomy* Nauka, Moscow [in Russian; English edition published by Harwood Academic Publishers, New York (1987)]
Wada, K., Baba, J., Saitoh, T. R. (2011) *Astrophys. J.* **735**, 1